Journal of Molecular Liquids 382 (2023) 121915

Contents lists available at ScienceDirect

Journal of Molecular Liquids

journal homepage: www.elsevier.com/locate/molliq

Chemical speciation of caffeic and *p*-coumaric acids with selected lanthanides

Edyta Nalewajko-Sieliwoniuk [a], Sofia Gama [a,b,*], Żaneta Arciszewska [a], Paulina Bogdan [a], Monika Naumowicz [c], Monika Kalinowska [d], Grzegorz Świderski [d], Renata Świsłocka [d], Włodzimierz Lewandowski [d,e], Gabriele Lando [f], Demetrio Milea [f,*], Beata Godlewska-Żyłkiewicz [a]

[a] Department of Analytical and Inorganic Chemistry, Faculty of Chemistry, University of Bialystok, K. Ciołkowskiego 1K, 15-245 Białystok, Poland
[b] Centro de Ciências e Tecnologias Nucleares, Instituto Superior Técnico, Universidade de Lisboa, Estrada Nacional 10 (km 1397), 2695-066, Bobadela LRS, Portugal
[c] Department of Physical Chemistry, Faculty of Chemistry, University of Bialystok, K. Ciołkowskiego 1K, 15-245 Białystok, Poland
[d] Department of Chemistry, Biology and Biotechnology, Bialystok University of Technology, Wiejska 45E, 15-351 Białystok, Poland
[e] Prof. Waclaw Dabrowski Institute of Agricultural and Food Biotechnology—State Research Institute, 36 Rakowiecka St., 02-532 Warsaw, Poland
[f] Dipartimento di Scienze Chimiche, Biologiche, Farmaceutiche ed Ambientali, CHIBIOFARAM, Università degli Studi di Messina, V.le F. Stagno d'Alcontres, 31, 98166 Messina, Italy

A B S T R A C T

Caffeic (CFA) and *p*-coumaric (*p*-CA) acids are biologically active compounds commonly found in plants and food of plant origin. Metal complexes of these acids exhibit diverse bioactivity, sometimes even higher than the free ligands. Lanthanide (Ln) complexes with organic ligands also attract the attention of researchers, due to their potential application as novel potential biologically active agents. The aim of the present study was the evaluation of the interactions of CFA and *p*-CA with representative lanthanides (Ln^{3+} = Eu^{3+}, Gd^{3+}, and Dy^{3+}) in aqueous solution. Potentiometric, spectrophotometric, and ^{1}H NMR techniques were used to study the acid-base behavior of CFA and *p*-CA, as well as their complexing ability towards Ln^{3+} cations, over a wide range of pH values ($2 \leq pH \leq 8$), in $KCl_{(aq)}$ at $I = 0.2$ mol dm^{-3} and $T = 298.15 \pm 0.1$ K. The evaluation of the sequestering ability of both ligands towards the studied lanthanides, by means of pM and $pL_{0.5}$ parameters, show that CFA is a better chelating agent.

1. Introduction

Hydroxycinnamic acids are phenylpropanoids, derivatives of cinnamic acid, biosynthesized as secondary metabolites by plants [1,2]. Among them, caffeic (CFA) and *p*-coumaric (*p*-CA) acids are the most representative (Scheme 1). *p*-CA is synthesized via the phenylpropanoid route, mainly from phenylalanine and tyrosine. It occurs in plants, both in free and conjugated form, forming derivatives of mono-, oligo- and polysaccharides, organic acids, and amines. *p*-CA can be found in fruits, vegetables, nuts, grains and mushrooms [3,4]. CFA is also one of the most common hydroxycinnamic acids, biosynthesized by hydroxylation of *p*-CA and found in vegetables, fruits, herbs, mushrooms, and plant-derived beverages (*e.g.*, wine and coffee) [2].

CFA and *p*-CA are known for their diverse physiological functions, including antioxidant, antibacterial, antitumor, anti-inflammatory, and antidiabetic activity, which leads to their use in many fields of industry, such as chemical, food, cosmetics, and pharmaceutical industry [1,4].

Lanthanides (Ln) are actively studied for their unique properties, in particular optical and magnetic [5,6]. The study of Ln complexes with organic ligands continuously attracts research interest, due to their potential application as electronic luminescent materials, biosensors, antimicrobial or anticancer drugs [7–9]. Their complexes are used, for example, as emission probes in optical spectroscopy and microscopy and as contrast agents in magnetic resonance imaging and angiography [10–12]. Furthermore, it has been reported that Ln complexes exhibit interesting biological activity [13–18]. In many countries (*e.g.*, China, Austria, Switzerland) Ln both in organic and inorganic forms are also applied in zootechnics and agriculture [19,20]. The complexation with Ln^{3+} could enhance antibacterial [10,15–18], antifungal [15,17], antioxidant [17] or anticancer [14] activity of free organic ligands, as well

* Corresponding authors at: Centro de Ciências e Tecnologias Nucleares, Instituto Superior Técnico, Universidade de Lisboa, Estrada Nacional 10 (km 1397), 2695-066 Bobadela LRS, Portugal (S. Gama); Dipartimento di Scienze Chimiche, Biologiche, Farmaceutiche ed Ambientali, CHIBIOFARAM, Università degli Studi di Messina, V.le F. Stagno d'Alcontres, 31, 98166 Messina, Italy (D. Milea).
E-mail addresses: sofia.gama@ctn.tecnico.ulisboa.pt (S. Gama), dmilea@unime.it (D. Milea).

https://doi.org/10.1016/j.molliq.2023.121915
Received 16 February 2023; Received in revised form 6 April 2023; Accepted 22 April 2023
Available online 2 May 2023
0167-7322/© 2023 The Author(s). Published by Elsevier B.V. This is an open access article under the CC BY-NC-ND license (http://creativecommons.org/licenses/by-nc-nd/4.0/).

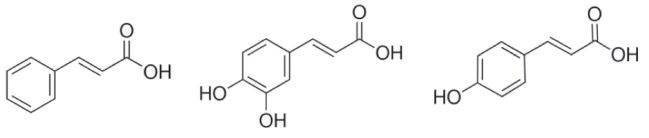

cinnamic acid caffeic acid (CFA) *p*-coumaric acid (*p*-CA)

Scheme 1. Chemical structure of cinnamic and hydroxycinnamic acids.

as the bioactivity of free metal ions [14–16].

Despite their importance, relatively few data are available for Ln^{3+} complexes with natural antioxidant molecules such as phenolic compounds [21,22] and there is very limited information in literature on the structure and the solution thermodynamic behavior of phenolic acids/Ln^{3+} complexes. In this context, the study of the coordination properties of Ln^{3+} in relation to natural antioxidant molecules may deserve great interest in the search for compounds that are safe for use by humans and can be applied in, for example, the food industry. Therefore, the main goal of the present study was the evaluation of the chelating ability of CFA and *p*-CA towards different Ln^{3+} (Eu^{3+}, Gd^{3+}, and Dy^{3+}).

2. Materials and methods

2.1. Reagents and solutions

Caffeic acid (3-(3,4-dihydroxyphenyl)-2-propenoic acid, CFA, H_3L), *p*-coumaric acid (4-hydroxycinnamic acid, *p*-CA, H_2L), europium(III) chloride hexahydrate ($EuCl_3{\cdot}6H_2O$), gadolinium(III) chloride hexahydrate ($GdCl_3{\cdot}6H_2O$), and dysprosium(III) chloride hexahydrate ($DyCl_3{\cdot}6H_2O$) were purchased from Sigma-Aldrich Chemie GmbH (Steinheim, Germany). Hydrochloric acid (HCl) TitraFix™, potassium hydroxide (KOH) TitraFix™, potassium chloride (KCl), ethylenediaminetetraacetic acid disodium salt dihydrate ($C_{10}H_{14}N_2Na_2O_8{\cdot}2H_2O$, EDTA) were purchased from POCH S.A. (Gliwice, Poland). KCl solutions were prepared by weighing the pure salt, previously dried in an oven at $T = 383.15$ K for two hours. The stock solutions of Eu^{3+}, Gd^{3+}, and Dy^{3+} ($c_M \approx 10$ mmol dm^{-3}) were obtained by dissolving an appropriate amount of salt in Milli-Q water (25 cm^3), and were standardized against standard EDTA solutions [23]. HCl and CO_2-free KOH solutions were prepared by diluting the concentrated TitraFix™ ampoules in Milli-Q water and standardized against tris (hydroxymethyl)aminomethane (Tris, ACS reagent, 99.8%, Sigma-Aldrich Chemie GmbH, Steinheim, Germany) and potassium hydrogen phthalate (Standard Reference Material, Merck, Germany), respectively, previously dried at $T = 383.15$ K for two hours. Soda lime traps were used to preserve the KOH solutions from atmospheric CO_2. All solutions were prepared in grade A glassware and with ultrapure water, obtained from a Milli-Q water purifying system (Millipore Direct-Q 3, Merck). All chemicals had an analytical purity and were used without further purification.

2.2. Potentiometric measurements

All potentiometric titrations were performed under an argon atmosphere, at the constant ionic strength of $I = 0.2$ mol dm^{-3} in $KCl_{(aq)}$ and at $T = 298.15 \pm 0.1$ K in thermostatted cells, using an Orion Star™ T910 Series Potentiometric Titrator (Thermo Scientific™) equipped with an automatic burette and a combined glass electrode Orion™ 8102BNUWP ROSS Ultra™ (Thermo Scientific™). The estimated accuracy was ±0.20 mV and ±0.001 cm^3 for potential readings and titrant volume additions, respectively.

Before each potentiometric titration, independent strong acid–strong base titrations were performed, in the same experimental conditions ($I = 0.2$ mol dm^{-3} in $KCl_{(aq)}$, $T = 298.15 \pm 0.1$ K) that were used for titrations of phenolic acid/complex solutions. These measurements were necessary for the determination of electrode potential (E^0) and the acidic junction potential ($E_j = j_a[H^+]$). Only in this way, the pH scale can be used, with pH = $-\log[H^+]$, where $[H^+]$ is the free proton concentration (not activity). p*K*w values were also calculated in order to evaluate the reliability of electrode calibration over the alkaline range [24–26]. For the determination of the acid–base properties of the free ligands (CFA and *p*-CA) and to study their interaction with Ln^{3+}, several potentiometric measurements were carried out by titrating 25 cm^3 of the titrand solution with standard KOH solutions, up to pH ≈ 8.0–8.5. Titrand solutions consisted of different amounts of ligand ($c_L \approx 1.0 - 1.3$ mmol dm^{-3}) and lanthanide cation ($c_{Ln} \approx 0.5$–1.3 mmol dm^{-3}) in different ratios ($1{:}1 \le c_M{:}c_L < 1{:}2$), HCl ($c_H \approx 2.0$–$5.0$ mmol dm^{-3}) and the necessary amount of $KCl_{(aq)}$ to reach the ionic strength of $I = 0.2$ mol dm^{-3}.

2.3. UV–Vis spectrophotometric measurements

UV–Vis spectrophotometric measurements were carried out with an Evolution One UV–Vis Spectrophotometer (Thermo Scientific™) equipped with an optical fiber probe, with a fixed 1 cm path length. The same conditions of temperature ($T = 298.15 \pm 0.1$ K, maintained by circulating thermostated water) and ionic strength ($I = 0.2$ mol dm^{-3} in $KCl_{(aq)}$) of potentiometric measurements were used. Several spectrophotometric UV–Vis titrations were carried out in the wavelength range of 220–450 nm by titrating 25 cm^3 of solutions containing the ligand (CFA or *p*-CA, $c_L \approx 4.0$–6.0×10^{-5} mol dm^{-3}), HCl ($c_H \approx 1.0$–2.0×10^{-3} mol dm^{-3}) and $KCl_{(aq)}$, with standardized KOH solutions, up to pH ≈ 12. The titrant additions and the potential readings were done with the same system used for potentiometric measurements. Also, the combined glass electrode was calibrated according to the procedure described before. To evaluate the formation of complexes of Ln^{3+} with both ligands and to determine the corresponding stability constants, several measurements were carried out on solutions prepared as above described, with suitable additions of Ln^{3+} to obtain different metal to ligand ratios ($1{:}1 \le c_M{:}c_L \le 1{:}3$).

2.4. ^{1}H NMR measurements

^{1}H NMR titrations were performed using a Bruker Avance II 400 spectrometer and were performed in solutions with a known ligand concentration ($c_L \approx 10^{-3}$ mol L^{-1}) in $KCl_{(aq)}$ at $I = 0.2$ mol dm^{-3} and $T = 298.15$ K, in 5 mm NMR tubes, following the procedure described in our previous works [27,28]. As an external reference, a D_2O capillary was introduced in each NMR tube, avoiding the preparation of the samples in H_2O/D_2O mixtures, as commonly done [29,30]. This was done to avoid the need for evaluation of the isotopic effect, as the binding affinities of protonating groups are slightly different for D^+ and H^+ [31,32]. In addition, a pre-saturation pulse sequence technique was used to suppress the residual water signal. A standardized KOH solution was used to adjust the pH, measured with a calibrated Orion™ 8103BNUWP ROSS Ultra™ semi-micro tipped glass combination electrode, calibrated as described above.

2.5. Thermodynamic calculations

The parameters of the electrode calibrations (E^0, pK_w, acidic junction potential coefficient j_a, analytical concentrations of reagents), the protonation constants of phenolic acids, and the stability constants of their Ln(III) complexes were determined by refinement of the experimental data using the non-linear least squares software BSTAC4 [33]. HypSpec2014 program was used to analyse the spectrophotometric data, and to determine the stability constants and the molar absorbance spectra of the absorbing species [34]. ^{1}H NMR data were analyzed by HypNMR [35], while ES4 [33] and HYSS [36] computer programs were applied to draw the speciation and the sequestration diagrams.

Table 1
Protonation constants of CFA and *p*-CA acids in $KCl_{(aq)}$ at $I = 0.2$ mol dm^{-3} and $T = 298.15$ K.

Species	(p:q:r)	log β_{pqr} [a] (log K_{01r}) [b] CFA [c]	*p*-CA
LH	0:1:1	11.93	9.028 ± 0.004
LH_2	0:1:2	20.59 (8.66)	13.401 ± 0.004 (4.37)
LH_3	0:1:3	24.92 (4.33)	–

[a] log β_{pqr} refer to the equilibrium: $p\ Ln^{3+} + q\ L^{z-} + r\ H^{+} = Ln_pL_qH_r^{(3p-zq+r)}$ ± SD
[b] log K_{01r} refer to the equilibrium: $H^{+} + LH_{r-1}^{(r-z-1)} = LH_r^{(r-z)}$.
[c] values from ref. [27].

The stability constants of complexes of Ln^{3+} with CFA and *p*-CA are expressed according to Eq. (1), considering the overall equilibrium:

$$p\ Ln^{3+} + q\ L^{z-} + r\ H^{+} = Ln_pL_qH_r^{(3p-zq+r)}\ \log\ \beta_{pqr} \quad (1)$$

The same equation is valid for the Ln^{3+} hydrolysis ($q = 0$ and $r < 0$) and ligand protonation constants ($p = 0$).

The stability constants, concentrations of reagents and ionic strength of solutions are expressed as the molar concentration (c, mol dm^{-3}), while uncertainties are presented as ±standard deviation (SD). For simplicity and when it is not relevant, the charges of the species are omitted.

2.6. Evaluation of the sequestering ability

The assessment of the sequestering ability of CFA and *p*-CA towards the investigated metal ions has been carried out by calculating a semi-empirical parameter, $pL_{0.5}$, which represents the total concentration of the ligand (L, as $-\log c_L$) required to bind 50 % (as mole fraction, $x_{M_L} = 0.5$) of a given metal ion (M) in a given solution when M is present as trace (in this case, for computational purposes, $c_M = 10^{-24}$ mol dm^{-3}). By plotting the fraction x_{M_L} of the metal bound only to L vs. $-\log c_L$, we obtain a sigmoidal curve (sequestration diagram) that can be fitted to Eq. (2), a Boltzmann-type equation, where $pL = -\log c_L$, and $pL_{0.5}$ is the only adjustable parameter.

$$x_{M_L} = \frac{1}{1 + 10^{(pL - pL_{0.5})}} \quad (2)$$

The higher the $pL_{0.5}$ value, the greater the sequestering ability of the evaluated ligand is. The method of calculating the $pL_{0.5}$ parameter shows the effective sequestering ability of a tested ligand L, representing the metal selectively taken up by the ligand, even in the presence of competing reactions. $pL_{0.5}$ can therefore be determined in systems of all possible complexity, in which many other metal cations and ligands are simultaneously present (*e.g.*, in biological and environmental samples). Bearing in mind that, the sequestering ability depends on the experimental conditions of the investigated system (*e.g.*, ionic strength, pH, temperature). For c_M approaching to zero (*i.e.*, at very low concentrations like those used in our calculations), $pL_{0.5}$ usually tends to become constant and can be used for comparison purposes. In fact, although Eq. (2) was not fully rigorous and was empirically derived from sequestration diagrams, it proved to be excellent for modelling, in terms of sequestration capacity, the behaviour of many systems of variable complexity. Further details about this parameter and information on how to calculate it can be found in refs. [26,37].

3. Results and discussion

3.1. Acid–Base properties of CFA and p-CA

For the determination of the stability constants of the Ln^{3+}/CFA and Ln^{3+}/*p*-CA complexes, it is necessary to know the acid–base properties of CFA and *p*-CA under the same experimental conditions. Table 1 shows the protonation constants of CFA, previously determined [27], while the same detailed study was performed in this work for *p*-CA, using potentiometric and UV–Vis spectrophotometric techniques, complemented by ^{1}H NMR studies.

Several independent potentiometric measurements were performed and, from the data obtained, we could determine the values of two protonation steps, corresponding to the protonation of the hydroxyl group in the *para* position of the aromatic ring and of the carboxylic acid, respectively. For a better characterization of the system, various UV–Vis spectrophotometric measurements were also done (see example in Fig. 1a). The spectra obtained for *p*-CA were processed by HypSpec software, allowing the simultaneous determination of both the protonation constants (log $\beta_{011} = 8.99 \pm 0.01$ and log $\beta_{012} = 13.20 \pm 0.01$, which are in very good agreement with the potentiometric results reported in Table 1) and the molar absorptivity spectra for each species (Fig. 1b). The fully protonated form of *p*-CA, LH_2, is characterized by an absorption band with a $\lambda_{max} = 310$ nm. With the increase of the pH, during the first step of deprotonation, a hypsochromic shift (blue shift) is observed, reaching λ_{max} at 283 nm for LH^-. Further pH increase leads then to a bathochromic shift (red shift), with the fully deprotonated species L^{2-}, characterized by a band with maximum absorption at $\lambda_{max} = 332$ nm.

Despite the fact that *p*-CA is a very well know molecule, a good assignment of the protonation steps cannot be done only using potentiometric and/or UV–Vis spectrophotometric techniques. Nevertheless, using similar molecules as reference, namely CFA, we can propose that the first protonation step occurs on the phenolate group (at pH around 8–9) and the second on the carboxylate (around pH 4), like in the case of CFA [27]. For a better insight into the system, ^{1}H NMR experiments were performed, as the change with pH of the chemical shifts of protons in the vicinity of (de)protonable proton can be very informative. For this

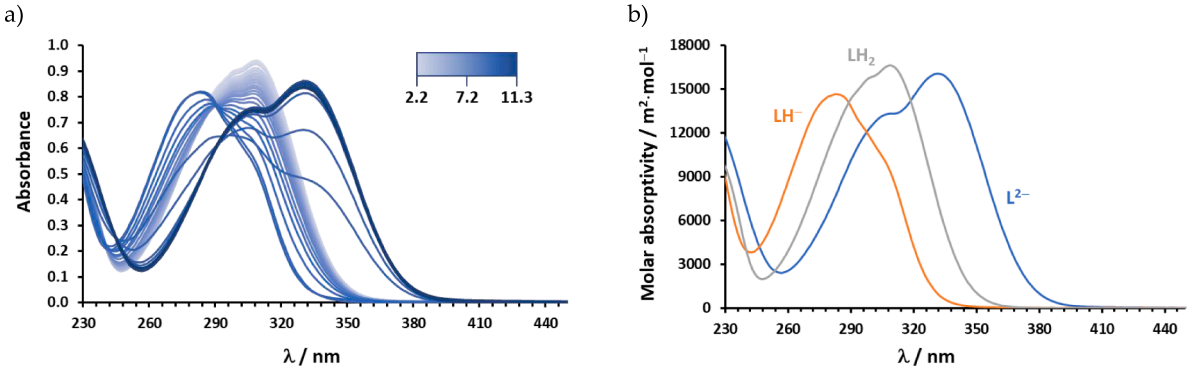

Fig. 1. a) Experimental representative absorption spectra of *p*-CA, measured at different pH values. $c_{p\text{-CA}} = 6 \times 10^{-5}$ mol dm^{-3}, in $KCl_{(aq)}$ at $I = 0.2$ mol dm^{-3} and $T = 298.15$ K; b) calculated molar absorptivity spectra of *p*-CA for LH_2, LH^-, and L^{2-} species.

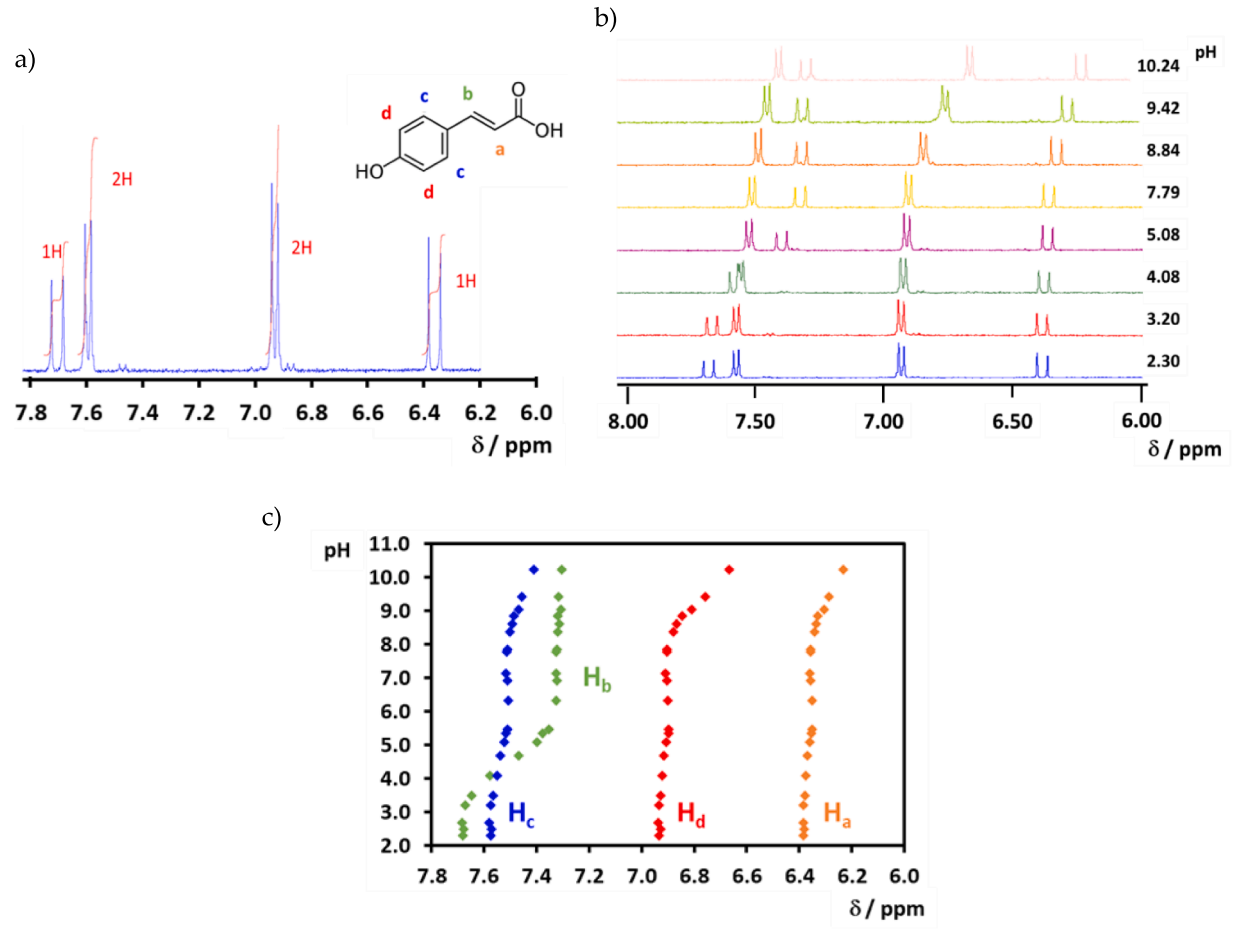

Fig. 2. ^{1}H NMR spectra obtained at different pH: a) *p*-CA spectra obtained at pH 2.30 with represented peak integrals and *p*-CA chemical structure with the corresponding ^{1}H NMR peak attribution; b) some representative ^{1}H NMR spectra of *p*-CA; c) graphical representation of the chemical shifts of each assigned peak obtained from the experimental spectra recorded at different pH values.

Table 2
Calculated chemical shift (δ /ppm) of different (de)protonated species of *p*-CA, in $KCl_{(aq)}$ at $I = 0.2$ mol dm^{-3} and $T = 298.15$ K.

	Nucleus			
Species	**H_b**	**H_c**	**H_d**	**H_a**
	δ /ppm			
L^{2-}	7.300	7.397	6.633	6.218
LH^{-}	7.323	7.512	6.904	6.357
LH_2	7.685	7.575	6.932	6.383

purpose, we measured the ^{1}H NMR spectra of different solutions of *p*-CA, prepared under the same conditions of potentiometric experiments, at different pH values. Some of the obtained spectra are presented in Fig. 2a and b. By plotting the chemical shifts of the signal of each proton vs. pH (Fig. 2c), we can observe that, at pH between ≈3 and 5, the peak of H_b shows a large change in its chemical shift to a higher field, and the same occurs at pH above 8 for H_d. As both observations result from the structural changes in the magnetic field around the mentioned protons due to the deprotonation processes, we can conclude that: *i*) the deprotonation of the carboxylic acid occurs between pH *ca.* 3–5, indicating a pK_a of around 4 (data processed by HypNMR gave log $K_{012} = 4.5 \pm 0.1$); *ii*) at higher pH values, the deprotonation process mainly affects the vicinity of proton H_d as the result of the deprotonation of the phenolic group (determining log $K_{011} = 9.37 \pm 0.03$ by HypNMR). By fitting the presented titration curves of chemical shift vs pH (Fig. 2c) we could also determine the chemical shifts of the assigned protons for the

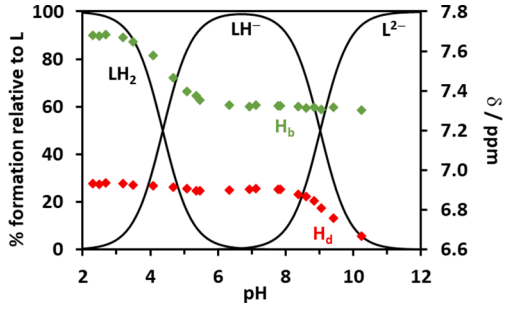

Fig. 3. Speciation diagram of *p*-CA species ($c_{p\text{-CA}} = 1$ mmol dm^{-3}) as a function of pH, in $KCl_{(aq)}$ at $I = 0.2$ mol dm^{-3} and $T = 298.15$ K, superimposed with the chemical shifts of assigned peaks.

different protonated/deprotonated species (see Table 2), as well as the calculated chemical shifts of each measured sample (see Table S1). It is worth mentioning that the determined log K_{011} and log K_{012} are slightly higher than the analogous values obtained by both potentiometric and UV–Vis spectrophotometric titrations. However, the uncertainty on the determined values is higher, also due to the objective limitations of the ^{1}H NMR technique in terms of the smaller number of recordable experimental points. Taking into account this aspect, it can be concluded that protonation constants obtained by ^{1}H NMR are still in good agreement with the values obtained in this work by the previously mentioned techniques, as well as with the literature (*e.g.*, Beltrán *et al.*

[38] reported log K_{011} = 8.98, log K_{012} = 4.36).

The obtained protonation constants were then used to draw the speciation diagram (Fig. 3), in which it is evident that the first deprotonation starts already at acidic pH, leading to the formation of the LH^{-} species, the main species at neutral pH. The deprotonation of the hydroxyl group starts at pH ≈ 8, resulting in the fully deprotonated L^{2-} species. The superimposition of the variation of the chemical shifts of H_b and H_d to the speciation diagram in Fig. 3 clearly evidence that the change observed on H_b is in line with the formation of LH^{-}, while H_d changes with the formation of L^{2-}, confirming the above statements about the deprotonation sequence of *p*-CA.

3.2. Acid–base properties of Ln^{3+} (hydrolysis)

As for the ligands, for the correct determination of the stability constants of the $Ln_pL_qH_r$ species in the studied systems, it is also necessary to know the acid-base properties of Ln^{3+} ions (*i.e.* their hydrolysis). Main hydrolysis reference books [39,40] report the formation of three main species, namely $[Ln(OH)]^{2+}$, $[Ln(OH)_2]^{+}$, and $Ln(OH)_3$. According to Brown and Eckberg [40], while $[Ln(OH)]^{2+}$ formation is well described in different experimental conditions, the same cannot be said for other species. For example, there are four reported values for the stability of $[Gd(OH)_2]^{+}$ [41–43] and three for the stability of $Gd(OH)_{3(aq)}$ [42,44], but none of the data appears to be consistent with the stability constant of $[Gd(OH)]^{2+}$ [40]. The same is reported in the case of Dy^{3+}: while for $[Dy(OH)]^{2+}$ there are several studies that present log β values in good agreement between them [45–47], there is only a single work that reports data for the stability of the higher monomeric hydrolysis constants of Dy^{3+} [44] where the proposed value for the stability constant of $Dy(OH)_{3(aq)}$ (log $\beta_{10\text{-}3}$) is greater than 3 × log $\beta_{10\text{-}1}$ [40]. In the case of Eu^{3+}, there are many reported values determined for log $\beta_{10\text{-}1}$, obtained in different experimental conditions of temperature and ionic strength, in good agreement among them. Nevertheless, also for Eu^{3+}, despite its hydrolysis is one of the most studied among lanthanides, only few studies report the hydrolysis constants of higher monomeric species, as $[Ln(OH)_2]^{+}$ and $[Ln(OH)_3]$ [44,48–50]. In all of them, values were considered as not reliable in the critical data revision done by Brown and Ekberg in 2016 [40], who thus suggest to just consider the formation of $[Ln(OH)]^{2+}$ species as reliable (*i.e.*, with reliable hydrolysis constants available).

As such, we decided in this work to follow the above recommendation, considering in our calculations only the hydrolysis constants of $[Eu(OH)]^{2+}$, $[Gd(OH)]^{2+}$, and $[Dy(OH)]^{2+}$ species, taking them from the work of Klungness and Byrne [46]. These authors determined the hydrolysis constants log $\beta_{10\text{-}1}$(Ln) of the all lanthanide series by potentiometric and spectrophotometric experiments in $NaClO_{4(aq)}$ at different temperatures (298.15 K, 313.15 K, and 328.15 K) and in a large ionic strength range (0.04 < *I*/mol dm^{-3} < 5.7). From this complete and accurate study, Klungness and Bryne derived an equation for the dependence of $[Ln(OH)]^{2+}$ hydrolysis constants on temperature (*T*) and ionic strength (*I*) for all the investigated Ln^{3+} cations in $NaClO_{4(aq)}$:

$$\log \beta_{10\text{-}1}(\mathrm{Ln}) = \log {}^{0}\beta_{10\text{-}1}(\mathrm{Ln}) - \{2.044\, I^{1/2}/(1 + 5.52\, I^{1/2}) - 1.84 \times 10^{-3}\, I - 2446\, K/T + 8.204 \quad (3)$$

with log ${}^{0}\beta_{10\text{-}1}$(Ln) as the hydrolysis constant of the corresponding $[Ln(OH)]^{2+}$ species at *T* = 298.15 K temperature and zero ionic strength [46]. In this work we thus used log $\beta_{10\text{-}1}$(Eu) = –8.02, log $\beta_{10\text{-}1}$(Gd) = –8.09 and log $\beta_{10\text{-}1}$(Dy) = –7.85, calculated using Eq. (3) at *I* = 0.2 mol dm^{-3}. It is worth to mention that, despite the fact that Eq. (3) was defined for $NaClO_{4(aq)}$ media, at such low ionic strength values (*I* = 0.2 mol dm^{-3}), the activity coefficient of La^{3+} in K/$NaCl_{(aq)}$ or $NaClO_{4(aq)}$ solutions, calculated from the Pitzer equations is very similar, as demonstrated by Millero [51], resulting in practically the same log β values in those media. More recent papers report values consistent with values calculated by Eq. (3) [50,52–55].

Table 3
Stability constants of $Ln_pL_qH_r$ species of CFA and *p*-CA in $KCl_{(aq)}$ at *I* = 0.2 mol dm^{-3} and *T* = 298.15 K.

Equilibrium	Species	(p:q:r)	log β_{pqr} [a]		
			Eu^{3+}	Gd^{3+}	Dy^{3+}
CFA					
Ln + L = LnL	LnL	1:1:0	10.52[b]	10.57 ± 0.01	11.03 ± 0.01
Ln + L = LnLOH + H	LnL(OH)	1:1:-1	0.03[b]	−0.24 ± 0.01[c]	−0.083 ± 0.002[c]
p-CA					
Ln + L + H = LnLH	LnLH	1:1:1	12.02 ± 0.01(2.99 ± 0.02) [d]	11.81 ± 0.01(2.78 ± 0.03) [d]	11.99 ± 0.01 (2.87 ± 0.04) [d]
Ln + L = LnL	LnL	1:1:0	4.15 ± 0.01 (3.14 ± 0.05) [e]	4.09 ± 0.01 (3.15 ± 0.06) [e]	5.17 ± 0.01 (3.99 ± 0.04) [e]

[a] log β_{pqr} refer to the equilibrium: pLn + qL + rH^{+} = $Ln_pL_qH_r$ ± SD.
[b] values from ref. [27].
[c] values obtained from spectrophotometric measurements.
[d] log *K* refer to the equilibrium Ln + LH = LnLH.
[e] log *K* correspondent to the equilibrium Ln(OH) + LH = LnLH(OH).

3.3. Speciation of the Ln^{3+}/CFA and Ln^{3+}/*p*-CA systems

For the determination of the stability constants of the different Ln^{3+}/L metal complexes several potentiometric and UV–Vis spectrophotometric independent titrations were performed.

Following the research undertaken in previous work on Eu^{3+}/CFA [27], we also evaluated the interactions of CFA with Gd^{3+} and Dy^{3+}. The analysis of potentiometric and UV–Vis spectrophotometric data indicates the formation of the same species for all three metal ions, namely LnL and $[LnL(OH)]^{-}$, where L = CFA and Ln = Gd^{3+} and Dy^{3+}. By potentiometry, due to the formation of sparingly soluble species, it was only possible to determine the stability of LnL species. By spectrophotometry, working at much lower concentrations, higher pH values could be reached without evident formation of precipitate, allowing the further determination of the $[LnL(OH)]^{-}$ hydroxo-species. The corresponding stability constants are reported in Table 3. Fig. 4 shows an example of spectrophotometric titration for the Dy^{3+}/CFA system. The obtained log β_{110} are in good agreement with the literature findings for the structurally similar ligand, catechol (log β_{110} = 10.88 for Eu^{3+}, log β_{110} = 10.74 for Gd^{3+} and log β_{110} = 10.60 for Dy^{3+}) [56].

Since only three metal cations were investigated in this work, it is not possible to infer about eventual regularities in the stability of CFA and *p*-CA complexes along the lanthanide series. Nevertheless, it is possible to affirm that slight differences observed in the stability constants given in Table 3 are, at least, consistent with the results of our previous studies on Ln^{3+} sequestering ability of other ligands, in which the stability of lanthanide complexes follow the so-called "tetrad", "double-double" effect or "gadolinium break" [57–59]. In this work, the stability of Gd^{3+} complexes with both CFA and *p*-CA is comparable (slightly lower) with that of Eu^{3+}, and lower than that of Dy^{3+}. Considering the interaction with CFA, this effect is better observed in the speciation diagrams (Fig. 5a), which show that the higher stability of DyL species results on its formation at slightly lower pH values (*ca.* pH 5.5 vs pH 6) than EuL or GdL (see solid and dashed lines, respectively, in Fig. 5a), with a higher percentage in solution over a larger pH range, leading also to the formation of the $[DyL(OH)]^{-}$ hydroxo species at higher pH (pH 10 vs pH 9).

The interaction of *p*-CA with Ln^{3+} turned out to be different when compared with that of CFA, due to the structural differences among the two ligands, which lead to different coordination modes. While for CFA the coordination most likely occurs via catecholate moiety, in the case of *p*-CA the carboxylate group seems to be involved in the coordination of lanthanide metal cations. This is in agreement with previous findings on the interaction of CFA and *p*-CA with other trivalent metal cations, such as Al^{3+} [60]. Moreover, this hypothesis is also supported by the

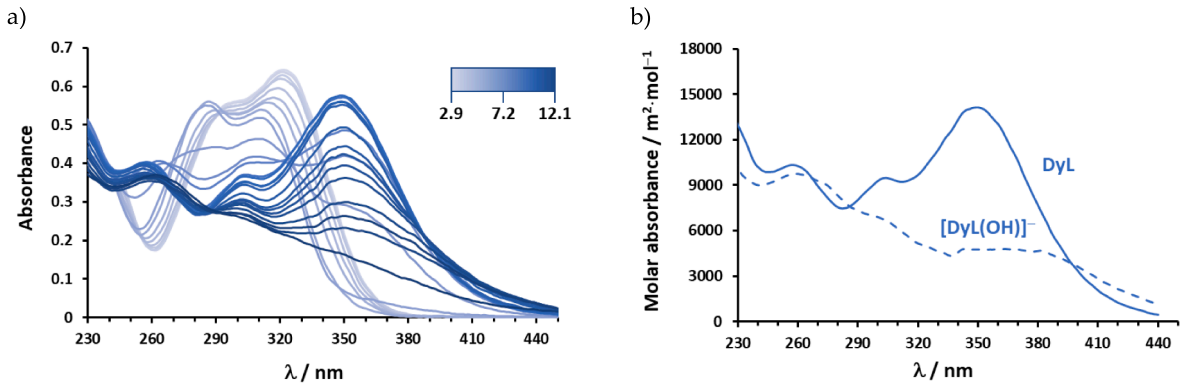

Fig. 4. A) experimental representative absorption spectra of dy^{3+}/CFA system, measured at different pH values and at 1:1 ratio, $c_{CFA} = c_{Dy} = 3.95 \times 10^{-5}$ mol dm^{-3}, in $I = 0.2$ mol dm^{-3} $KCl_{(aq)}$ and $T = 298.15$ K; b) Calculated molar absorptivity spectra of [DyL] and $[DyL(OH)]^-$ species, L = CFA.

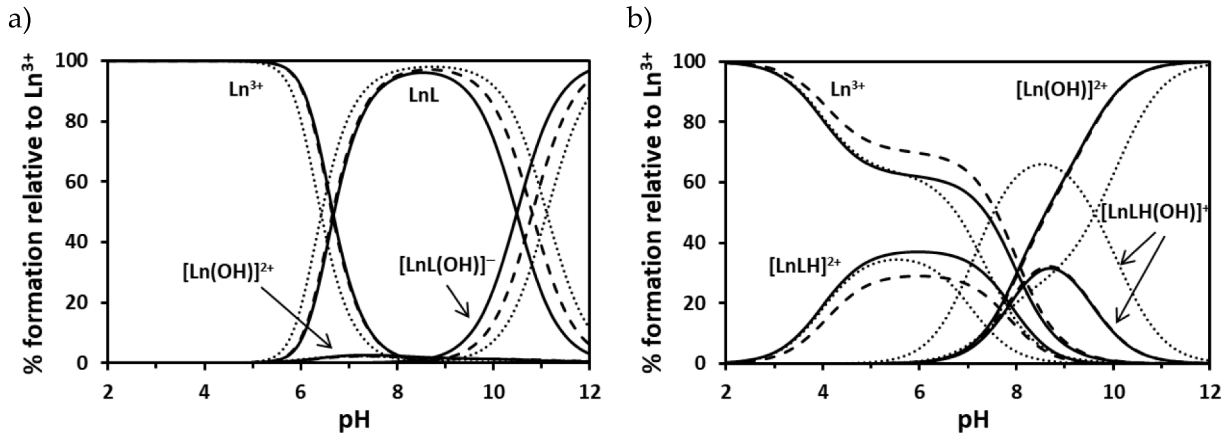

Fig. 5. Speciation diagrams of the $Ln_pL_qH_r$ species as a function of pH in the a) Ln^{3+}/CFA and b) Ln^{3+}/*p*-CA systems ($c_L = c_{Ln3+} = 1$ mmol dm^{-3}), where $Ln^{3+} = Eu^{3+}$, Gd^{3+}, and Dy^{3+} species represented by solid, dashed, and dotted lines, respectively.

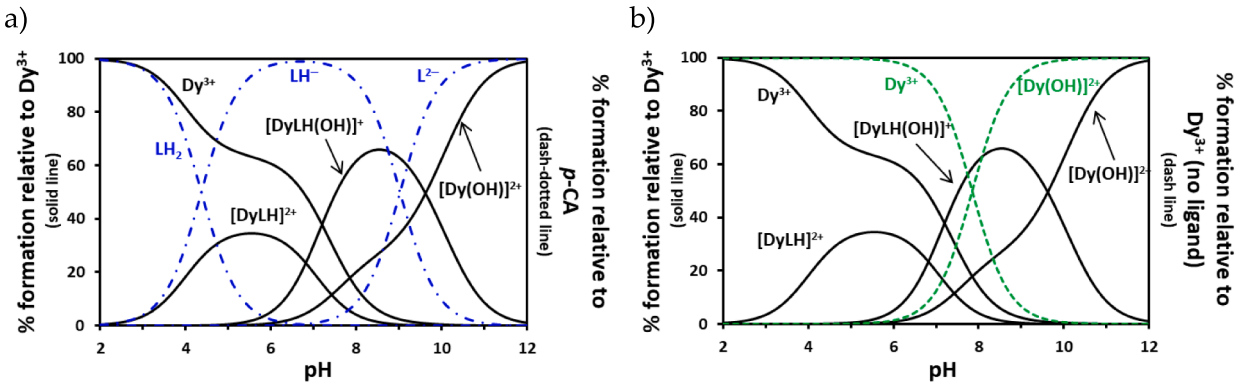

Fig. 6. Speciation diagrams of the $Dy_pL_qH_r$ species as a function of pH in the Dy^{3+}/*p*-CA system, overlapped with the speciation diagram of a) *p*-CA ligand (blue dashed lines) and b) Dy^{3+} (green dashed lines) ($c_{p\text{-CA}} = c_{Ln3+} = 1$ mmol dm^{-3}).

proposed speciation models and the stability constants of the species. In particular, it is worth to pay attention to the ligand's and cation's species effectively involved in the complex formation reaction. Table 3 reports two distinct equilibria for the formation of the LnL^+ species. In fact, LnL^+ species can be formed as the result of the interaction between the free metal cation (Ln^{3+}) and the free ligand (L^{2-}), or between the protonated ligand and the hydrolysed cation. Though both equilibria are perfectly equivalent concerning the final product, and no direct information can be obtained by the above techniques for the species effectively involved in the formation reaction of the "final" complex [61–63], some speculation can be done. The LnL species starts to form at pH ≈ 6 (Fig. 6), where the phenolate of *p*-CA is still protonated (*i.e., p*-CA is present as LH^+, deprotonation starts at pH > 8). In those conditions, the coordination of the metal cation to the ligand to form the LnL species would involve, like in the case of a strong metal-to-ligand binding, the displacement of the proton that, considering the formation pH of the LnL

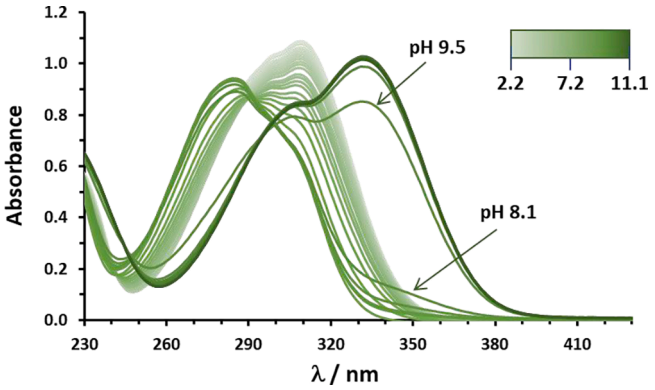

Fig. 7. Experimental representative absorption spectra of Gd^{3+}/*p*-CA system, measured at different pH values and at 1:1 ratio, $c_{p\text{-CA}} = c_{Gd} = 6 \times 10^{-5}$ mol dm^{-3}, in $I = 0.2$ mol dm^{-3} $KCl_{(aq)}$ and $T = 298.15$ K.

species, would necessarily be that of the phenolate group. However, proton displacement can only occur if the stability constant of the complex (*i.e.*, the binding of the metal cation) is comparable (or higher) with that of the (de)protonation equilibrium (this happens, for example, in the case of CFA). As can be noted, comparing log β_{LnL} values in Table 3 with the first protonation constant of *p*-CA (Table 1), this is not the case. As such, a different equilibrium seems to take place in our systems. By taking into account that the metal cations start to hydrolyse (forming $[Ln(OH)]^{2+}$, Ln = Eu^{3+}, Gd^{3+}, and Dy^{3+}) roughly in the same pH range of the LnL species, this let us suppose that the real reaction occurring in solution is, of the two above proposed, that one involving the monoprotonated *p*-CA and the hydrolysed lanthanide, according to equilibrium Ln(OH) + LH = LnLH(OH), as described in Table 3. Overall, the interaction of *p*-CA with the studied lanthanides can be explained as follows: at acidic pH, the lanthanide cation binds to the monoprotonated ligand, coordinating through the carboxylate, forming $[LnLH]^{2+}$. Once the metal complex is formed, the hydrolytic process of the metal cation occurs anyway leading to the formation of $[LnLH(OH)]^{+}$ (stoichiometrically represented as LnL). Furthermore, the $[LnLH]^{2+}$ species starts to form in the same pH range where the deprotonation process of the carboxylic moiety starts (pH 3–4).

As a further indication of the coordination of *p*-CA by the carboxylate group, it is worth mentioning that the order of magnitude of the determined formation constants is in full agreement with the literature values for similar ligands, such as phenylacetic (log $\beta_{110} = 2.06$ for Eu^{3+}, log $\beta_{110} = 1.96$ for Gd^{3+}, and log $\beta_{110} = 1.96$ for Dy^{3+}) and hydroxycinnamic acid (log $\beta_{110} = 2.18$ for Eu^{3+} and log $\beta_{110} = 1.96$ for Dy^{3+}) [56,64].

To get further insight into the system, mainly on the coordination mode, we also performed UV–Vis spectrophotometric titrations. Due to the experimental limitations of working at relatively low ligand concentrations (both for solubility reasons and eventually too high absorbance readings) as well as because more diluted titrant solutions cannot be used (*i.e.*, due to the accuracy of standardization, significant pH differences among each titration point, extreme dilution of the titrand solution, etc.), it was not possible to determine the stability constants of those species with sufficient accuracy. In fact, in the experimental conditions of the Ln^{3+}/*p*-CA systems, in which the stability of the complex species is relatively low, a significant pH jump was inevitably observed in the range where such species are formed, hampering the collection of a sufficient number of experimental data points in that range. This is better visualized in Fig. 7, which shows an example of UV/Vis titration for the Gd^{3+}/*p*-CA system.

Finally, for a global assessment of the sequestering ability of the two investigated ligands towards the three studied lanthanides, pM and $pL_{0.5}$ values were calculated. The use of these parameters is particularly suitable for comparisons between ligands with different acid-base properties and binding abilities, since in this case this information is not directly achievable from a simple assessment of the stability constants of the species formed [26]. The ability of both *p*-CA and CFA to sequester lanthanides cations is not too high, as demonstrated by the analysis of calculated pM values ($6.1 \leq pM \leq 6.5$), which are also in line with pM of Ln^{3+}/catechol or Ln^{3+}/phenylacetic acid systems (Fig. 8). Nevertheless, a slightly higher affinity is observed for CFA when compared with catechol, especially towards Dy^{3+} (6.46 vs 6.13).

Although, as originally defined by Raymond and co-workers [65], pM values are calculated at pH = 7.4, $pL_{0.5}$ can be estimated in very different conditions, even at various pH. Fig. 9 shows the sequestration diagrams calculated at different pH values for the Dy^{3+}/CFA (Fig. 9a) and Dy^{3+}/*p*-CA (Fig. 9b) systems. While, for CFA, $pL_{0.5}$ increase with pH (indicating a higher sequestering ability for higher pH values), for *p*-CA they increase until pH ≈ 8 and then decrease, as a clear indication that the formation of lanthanide-hydroxo species is favored over the complex (as also evidenced in the speciation diagrams presented in Fig. 6). The sequestration diagrams of the other systems are presented in the supplementary material (Fig. S1). Considering $pL_{0.5}$ values we can easily observe that, at pH 7.4, CFA has a better sequestering ability than *p*-CA towards the studied Ln^{3+} (Fig. 8c).

4. Conclusions

The chemical speciation of CFA and *p*-CA in the presence of three different Ln^{3+} (Eu^{3+}, Gd^{3+}, and Dy^{3+}) was evaluated in $KCl_{(aq)}$ at $I = 0.2$ mol dm^{-3} and $T = 298.15$ K. All the three investigated Ln^{3+} form two species with CFA, namely LnL and $[LnL(OH)]^{-}$, while LnLH and LnL^{+} are observed for *p*-CA. For each ligand, the stability of species with the

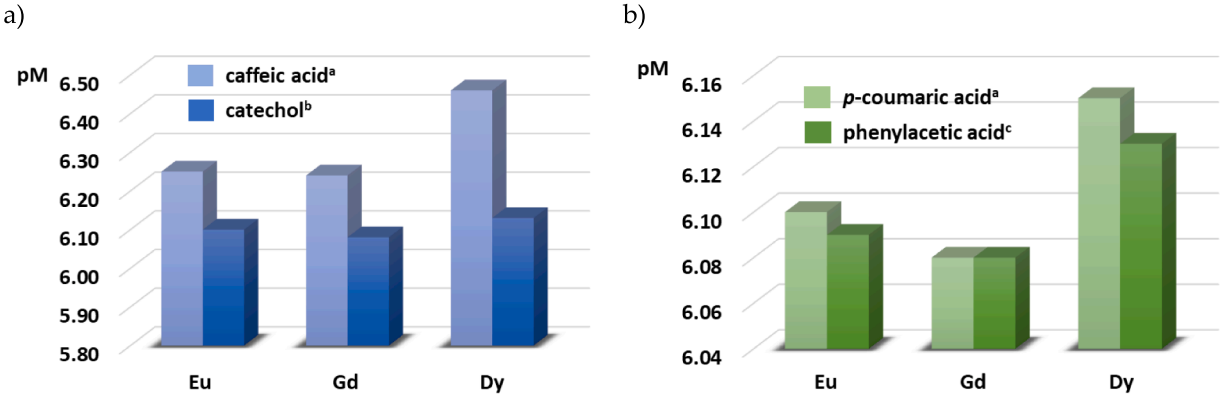

Fig. 8. Graphical representation of the pM values calculated at the recommended conditions (pH = 7.4 and $c_L = 10\ c_{Ln}$ with $c_L = 1 \times 10^{-5}$ mol dm^{-3} [65]) using data a) determined in this work and reported in ref. [27], b) ref. [56] and c) ref. [64].

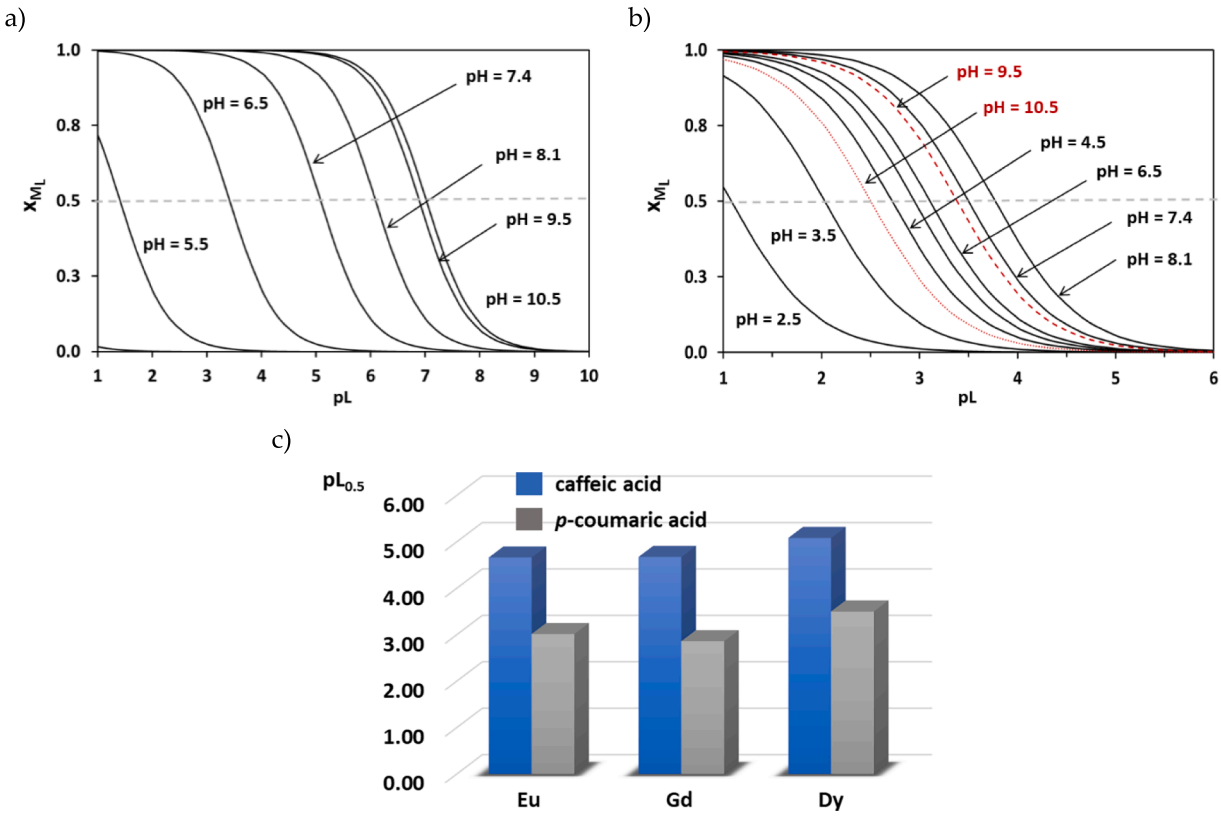

Fig. 9. Sequestration diagrams of Dy^{3+} by a) CFA and b) *p*-CA at different pH values, in $KCl_{(aq)}$ at $I = 0.2$ mol dm^{-3} and $T = 298.15$ K. c) $pL_{0.5}$ values calculated at pH 7.4 for the indicated Ln^{3+}/CFA and Ln^{3+}/*p*-CA systems.

same stoichiometry is comparable for the three investigated cations. Obtained results support the hypothesis that Ln^{3+} coordination occurs via catecholate group for CFA, and via the carboxylate moiety in the case of *p*-CA. Finally, CFA presents a slightly higher sequestering ability towards Ln^{3+} than *p*-CA, considering both pM and $pL_{0.5}$ parameters.

CRediT authorship contribution statement

Edyta Nalewajko-Sieliwoniuk: Investigation, Writing – original draft, Writing – review & editing, Visualization. **Sofia Gama:** Conceptualization, Methodology, Validation, Formal analysis, Data curation, Writing – original draft, Writing – review & editing, Supervision, Project administration. **Żaneta Arciszewska:** Investigation, Writing – original draft. **Paulina Bogdan:** Investigation. **Monika Naumowicz:** Conceptualization, Investigation, Visualization. **Monika Kalinowska:** Conceptualization, Resources, Visualization. **Grzegorz Świderski:** Investigation. **Renata Świsłocka:** Investigation, Visualization. **Włodzimierz Lewandowski:** Resources, Funding acquisition. **Gabriele Lando:** Methodology, Validation, Formal analysis, Data curation. **Demetrio Milea:** Conceptualization, Methodology, Validation, Formal analysis, Data curation, Writing – review & editing, Supervision, Project administration. **Beata Godlewska-Żyłkiewicz:** Conceptualization, Resources, Writing – review & editing, Supervision, Project administration, Funding acquisition.

Declaration of Competing Interest

The authors declare that they have no known competing financial interests or personal relationships that could have appeared to influence the work reported in this paper.

Data availability

Data will be made available on request.

Acknowledgements

The authors thank the National Science Centre (NCN), Poland, for the financing under the research project number 2018/29/B/NZ9/01997. This publication is also based upon work from COST Action CA18202—NECTAR—Network for Equilibria and Chemical Thermodynamics Advanced Research, supported by COST (European Cooperation in Science and Technology). SG and DM would also like to thank Prof. Giuseppe Gattuso from the University of Messina for the helpful discussion on ^{1}H NMR spectra interpretation.

Appendix A. Supplementary material

Supplementary data to this article can be found online at https://doi.org/10.1016/j.molliq.2023.121915.

References

[1] O. Taofiq, A.M. González-Paramás, M.F. Barreiro, I.C.F.R. Ferreira, Hydroxycinnamic acids and their derivatives: Cosmeceutical significance, challenges and future perspectives, a review, Molecules 22 (2017) 281.
[2] B. Godlewska-Żyłkiewicz, R. Świsłocka, M. Kalinowska, A. Golonko, G. Świderski, Ż. Arciszewska, E. Nalewajko-Sieliwoniuk, M. Naumowicz, W. Lewandowski, Biologically active compounds of plants: Structure-related antioxidant, microbiological and cytotoxic activity of selected carboxylic acids, Materials 13 (2020) 4454.
[3] K. Pei, J. Ou, J. Huang, S. Ou, p-Coumaric acid and its conjugates: dietary sources, pharmacokinetic properties and biological activities, J. Sci. Food Agric. 96 (2016) 2952.
[4] G. Granata, G.M.L. Consoli, R. Lo Nigro, C. Geraci, Hydroxycinnamic acids loaded in lipid-core nanocapsules, Food Chem. 245 (2018) 551.

[5] Ż. Arciszewska, S. Gama, B. Leśniewska, J. Malejko, E. Nalewajko-Sieliwoniuk, E. Zambrzycka-Szelewa, B. Godlewska-Żyłkiewicz, The translocation pathways of rare earth elements from the environment to the food chain and their impact on human health, Process Saf. Environ. Prot. 168 (2022) 205.
[6] J.-C.-G. Bünzli, S.V. Eliseeva, Intriguing aspects of lanthanide luminescence, Chem. Sci. 4 (2013) 1939.
[7] K. Zhou, Z. Feng, J. Shen, B. Wu, X. Luo, S. Jiang, L. Li, X. Zhou, Spectra, energy levels, and energy transition of lanthanide complexes with cinnamic acid and its derivatives, Spectrochim. Acta A Mol. Biomol. Spectrosc. 158 (2016) 29.
[8] H. Tsukube, S. Shinoda, Lanthanide complexes in molecular recognition and chirality sensing of biological substrates, Chem. Rev. 102 (2002) 2389.
[9] J.-C.-G. Bünzli, Lanthanide luminescence for biomedical analyses and imaging, Chem. Rev. 110 (2010) 2729.
[10] M. Birka, C.A. Wehe, O. Hachmöller, M. Sperling, U. Karst, Tracing gadolinium-based contrast agents from surface water to drinking water by means of speciation analysis, J. Chromatogr. A 1440 (2016) 105.
[11] J. Wahsner, E.M. Gale, A. Rodríguez-Rodríguez, P. Caravan, Chemistry of MRI contrast agents: Current challenges and new frontiers, Chem. Rev. 119 (2019) 957.
[12] M.C. Heffern, L.M. Matosziuk, T.J. Meade, Lanthanide probes for bioresponsive imaging, Chem. Rev. 114 (2014) 4496.
[13] I. Cota, V. Marturano, B. Tylkowski, Ln complexes as double faced agents: Study of antibacterial and antifungal activity, Coord. Chem. Rev. 396 (2019) 49.
[14] H.-H. Zou, T. Meng, Q. Chen, Y.-Q. Zhang, H.-L. Wang, B. Li, K. Wang, Z.-L. Chen, F. Liang, Bifunctional mononuclear dysprosium complexes: Single-ion magnet behaviors and antitumor activities, Inorg. Chem. 58 (2019) 2286.
[15] R. Fouad, Synthesis and characterization of lanthanide complexes as potential therapeutic agents, J. Coord. Chem. 73 (2020) 2015.
[16] S. Paswan, A. Anjum, N. Yadav, N. Jaiswal, R.K.P. Singh, Synthesis, thermal, photo-physical, and biological properties of mononuclear Yb3+, Nd3+, and Dy3+ complexes derived from Schiff base ligands, J. Coord. Chem. 73 (2020) 686.
[17] Z.A. Taha, A.K. Hijazi, W.M. Al Momani, Lanthanide complexes of the tridentate Schiff base ligand salicylaldehyde-2- picolinoylhydrazone: Synthesis, characterization, photophysical properties, biological activities and catalytic oxidation of aniline, J. Mol. Struct. 1220 (2020), 128712.
[18] Z.A. Taha, T.S. Ababneh, A.K. Hijazi, S.M. Al-Aqtash, W.M. Al-Momani, I. Mhaidat, Synthesis, spectral characterization, thermal, computational and antibacterial studies of lanthanide complexes with 2-fluorobenzoic acid-(5-R-2-hydroxy-benzylidene)hydrazide {R = chloro or bromo), J. Saudi Chem. Soc. 26 (2022), 101400.
[19] L. Cai, Y.S. Park, S.I. Seong, S.W. Yoo, I.H. Kim, Effects of rare earth elements-enriched yeast on growth performance, nutrient digestibility, meat quality, relative organ weight, and excreta microflora in broiler chickens, Livestock Sci. 172 (2015) 43.
[20] D. Carpenter, C. Boutin, J.E. Allison, J.L. Parsons, D.M. Ellis, Uptake and effects of six rare earth elements (REEs) on selected native and crop species growing in contaminated soils, PLoS One 10 (2015) e0129936.
[21] M.A. Lutoshkin, A.I. Petrov, A.S. Kazachenko, B.N. Kuznetsov, V.A. Levdansky, Complexation of rare earth metals by quercetin and quercetin-5'-sulfonic acid in acidic aqueous solution, Main Group Chem. 17 (2018) 17.
[22] M.A. Lutoshkin, I.V. Taydakov, B.N. Kuznetsov, Behavior of some perfluorinated analogs of thenoyltrifluoroacetone in aqueous solution, J. Chem. Eng. Data 64 (2019) 2593.
[23] H.A. Flaschka, EDTA titrations - an introduction to theory and practice, 2nd ed., Pergamon Press, 1964.
[24] R.M. Cigala, M. Cordaro, F. Crea, C. De Stefano, V. Fracassetti, M. Marchesi, D. Milea, S. Sammartano, Acid–base properties and alkali and alkaline earth metal complex formation in aqueous solution of diethylenetriamine-N, N, N′, N″, N″-pentakis(methylenephosphonic acid) obtained by an efficient synthetic procedure, Ind. Eng. Chem. Res. 53 (2014) 9544.
[25] S. Gama, M. Frontauria, N. Ueberschaar, G. Brancato, D. Milea, S. Sammartano, W. Plass, Thermodynamic study on 8-hydroxyquinoline-2-carboxylic acid as a chelating agent for iron found in the gut of Noctuid larvae, New J. Chem. 42 (2018) 8062.
[26] S. Gama, R. Hermenau, M. Frontauria, D. Milea, S. Sammartano, C. Hertweck, W. Plass, Iron coordination properties of Gramibactin as model for the new class of diazeniumdiolate based siderophores, Chem. Eur. J. 27 (2021) 2724.
[27] Ż. Arciszewska, S. Gama, M. Kalinowska, G. Świderski, R. Świsłocka, E. Gołębiewska, M. Naumowicz, M. Worobiczuk, A. Cudowski, A. Pietryczuk, C. De Stefano, D. Milea, W. Lewandowski, B. Godlewska-Żyłkiewicz, Int. J. Mol. Sci. 23 (2022) 888.
[28] P. Cardiano, R.M. Cigala, M. Cordaro, C. De Stefano, D. Milea, S. Sammartano, On the complexation of metal cations with "pure" diethylenetriamine-N, N, N′, N″, N″-pentakis(methylenephosphonic) acid, New J. Chem. 41 (2017) 4065.
[29] P. Cardiano, C. Foti, O. Giuffrè, On the interaction of N-acetylcysteine with Pb2+, Zn2+, Cd2+ and Hg2+, J. Mol. Liq. 223 (2016) 360.
[30] P. Cardiano, C. Foti, F. Giacobello, O. Giuffrè, S. Sammartano, Study of Al3+ interaction with AMP, ADP and ATP in aqueous solution, Biophys. Chem. 234 (2018) 42.
[31] A.K. Covington, M. Paabo, R.A. Robinson, R.G. Bates, Use of the glass electrode in deuterium oxide and the relation between the standardized pD (paD) scale and the operational pH in heavy water, Anal. Chem. 40 (1968) 700.
[32] M. Amélia Santos, S. Gama, L. Gano, G. Cantinho, E. Farkas, A new bis(3-hydroxy-4-pyridinone)-IDA derivative as a potential therapeutic chelating agent. Synthesis, metal-complexation and biological assays, Dalton Trans. 21 (2004) 3772.
[33] C. De Stefano, S. Sammartano, P. Mineo, C. Rigano, in: A. Gianguzza, Pelizzetti, E., Sammartano, S. (ed.) Marine Chemistry - an environmental analytical chemistry approach, Kluwer Academic Publishers, Amsterdam, The Netherlands, 1997, p. 71–83.
[34] P. Gans, A. Sabatini, A. Vacca, http://www.hyperquad.co.uk, 2008.
[35] C. Frassineti, S. Ghelli, P. Gans, A. Sabatini, M.S. Moruzzi, A. Vacca, Nuclear magnetic resonance as a tool for determining protonation constants of natural polyprotic bases in solution, Anal. Biochem. 231 (1995) 374.
[36] L. Alderighi, P. Gans, A. Ienco, D. Peters, A. Sabatini, A. Vacca, Hyperquad simulation and speciation (HySS): A utility program for the investigation of equilibria involving soluble and partially soluble species, Coord. Chem. Rev. 184 (1999) 311.
[37] F. Crea, C.D. Stefano, C. Foti, D. Milea, S. Sammartano, Chelating agents for the sequestration of mercury(II) and monomethyl mercury(II), Curr. Med. Chem. 21 (2014) 3819.
[38] J.L. Beltrán, N. Sanli, G. Fonrodona, D. Barrón, G. Özkan, J. Barbosa, Spectrophotometric, potentiometric and chromatographic pKa values of polyphenolic acids in water and acetonitrile–water media, Anal. Chim. Acta 484 (2003) 253.
[39] C.F. Baes, R.S. Mesmer, The hydrolysis of cations, Wiley, New York, 1976.
[40] P.L. Brown, C. Ekberg, in: Hydrolysis of metal ions, Wiley-VCH Verlag GmbH & Co. KGaA, Weinheim, Germany, 2016, pp. 225–324.
[41] A. Moutte, R. Guillaumont, Complexes citriques d'actinium et de curium, Rev. Chim. Miner. 6 (1969) 603.
[42] J. Kragten, L.G. Decnop-Weever, Hydroxide complexes of lanthanides—III Gadolinium(III) in perchlorate medium, Talanta 27 (1980) 1047.
[43] L.G. Rodenas, S.J. Liberman, Hydrolysis of gadolinium(III) in light and heavy water, Talanta 38 (1991) 313.
[44] N. Fatin-Rouge, J.-C.-G. Bünzli, Thermodynamic and structural study of inclusion complexes between trivalent lanthanide ions and native cyclodextrins, Inorg. Chim. Acta 293 (1999) 53.
[45] U.K. Frolova, V.N. Kumok, V.V. Serebrennikov, Hydrolysis of rare earth elements and yttrium in aqueous solutions, Izv. Vys. Ucheb. Zaved. Khim. 9 (1966) 176.
[46] G.D. Klungness, R.H. Byrne, Comparative hydrolysis behavior of the rare earths and yttrium: The influence of temperature and ionic strength, Polyhedron 19 (2000) 99.
[47] E. Vasca, D. Ferri, C. Manfredi, F. Fantasma, T. Caruso, C. Fontanella, S. Vero, On the hydrolysis of the dysprosium(III) ion, Chem. Spec. Bioaval. 16 (2004) 71.
[48] G.M. Nair, K. Chander, J.K. Joshi, Hydrolysis constants of plutonium(lll) and americium(lll), Radiochim. Acta 30 (1982) 37.
[49] M. F. Bernkopf, Hydrolysereaktionen und arbonatkomplexierung von dreiwertigem americium im natürlichen aquatischen systemen, Technische Universität München, 1990, Germany.
[50] E. Bentouhami, G.M. Bouet, J. Meullemeestre, F. Vierling, M.A. Khan, Physicochemical study of the hydrolysis of rare-earth elements (III) and thorium (IV), C. R. Chim. 7 (2004) 537.
[51] F.J. Millero, Stability constants for the formation of rare earth-inorganic complexes as a function of ionic strength, Geochim. Cosmochim. Acta 56 (1992) 3123.
[52] Y.Y. Yakubovich, V.G. Alekseev, Hydrolysis constants of tervalent lanthanum and lanthanide ions in 0.1 M KNO3 solution, Russ. J. Inorg. Chem. 57 (2012) 911.
[53] J. Schijf, R.H. Byrne, Speciation of yttrium and the rare earth elements in seawater: Review of a 20-year analytical journey, Chem. Geol. 584 (2021), 120479.
[54] M. Taha, I. Khan, J.A.P. Coutinho, Complexation and molecular modeling studies of europium(III)–gallic acid–amino acid complexes, J. Inorg. Biochem. 157 (2016) 25.
[55] M. Zabiszak, M. Nowak, Z. Hnatejko, J. Grajewski, K. Ogawa, M.T. Kaczmarek, R. Jastrzab, Thermodynamic and spectroscopic studies of the complexes formed in tartaric acid and lanthanide(III) ions binary systems, Molecules 25 (2020) 1121.
[56] D. Pettit, K. Powell, IUPAC Stability Constants Database, Academic Software, UK, Otley, 2004.
[57] H. Sigel, Metal Ions in Biological Systems, CRC Press, 2003.
[58] F. Crea, C. De Stefano, D. Milea, S. Sammartano, Thermodynamic data for lanthanoid(III) sequestration by phytate at different temperatures, Monatsh. Chem. 141 (2010) 511.
[59] R.M. Cigala, C. De Stefano, A. Irto, D. Milea, S. Sammartano, Thermodynamic data for the modeling of lanthanoid(III) sequestration by reduced glutathione in aqueous solution, J. Chem. Eng. Data 60 (2015) 192.
[60] A. Beneduci, E. Furia, N. Russo, T. Marino, Complexation behaviour of caffeic, ferulic and p-coumaric acids towards aluminium cations: a combined experimental and theoretical approach, New J. Chem. 41 (2017) 5182.
[61] K. Arena, G. Brancato, F. Cacciola, F. Crea, S. Cataldo, C. De Stefano, S. Gama, G. Lando, D. Milea, L. Mondello, A. Pettignano, W. Plass, S. Sammartano, 8-Hydroxyquinoline-2-carboxylic acid as possible molybdophore: A multi-technique approach to define Its chemical speciation, coordination and sequestering ability in aqueous solution, Biomolecules 10 (2020) 930.
[62] F. Crea, C.D. Stefano, D. Milea, S. Sammartano, Phytate–molybdate(VI) interactions in NaCl(aq) at different ionic strengths: Unusual behaviour of the protonated species, New J. Chem. 42 (2018) 7671.
[63] M.A. Santos, S. Gama, J.C. Pessoa, M.C. Oliveira, I. Tóth, E. Farkas, Complexation of molybdenum(VI) with bis(3-hydroxy-4-pyridinone)amino acid derivatives, Eur. J. Inorg. Chem. 2007 (2007) 1728.
[64] A.E. Martell, R.M. Smith, R.J. Motekaitis, NIST, NIST, Gaithersburg, 2004.
[65] W.R. Harris, C.J. Carrano, S.R. Cooper, S.R. Sofen, A.E. Avdeef, J.V. McArdle, K. N. Raymond, Coordination chemistry of microbial iron transport compounds. 19. Stability constants and electrochemical behavior of ferric enterobactin and model complexes, J. Am. Chem. Soc. 101 (1979) 6097.